7-Difluoromethoxyl-5,4'-di-n-octylygenistein targets the STAT3 pathway by upregulating microRNA-152-3p expression to inhibit self-renewal and tumor growth in non-small cell lung carcinoma

QING YUAN[1-3], XIANG LI[3], XUEMEI CHEN[4], JIANHUI XIAO[1,2] and JIANSONG ZHANG[3]

[1]Institute of Medicinal Biotechnology, Affiliated Hospital of Zunyi Medical University, Zunyi, Guizhou 563003, P.R. China; [2]Guizhou Provincial Key Laboratory of Medicinal Biotechnology and Research Center for Translational Medicine in Colleges and Universities, Affiliated Hospital of Zunyi Medical University, Zunyi, Guizhou 563003, P.R. China; [3]Department of Preclinical Medicine, Medical College, Hunan Normal University, Changsha, Hunan 410013, P.R. China; [4]Department of Pediatrics, Affiliated Hospital of Zunyi Medical University, Zunyi, Guizhou 563003, P.R. China

Received October 27, 2024; Accepted February 25, 2025

DOI: 10.3892/or.2025.8899

Abstract. MicroRNAs (miRs) serve a pivotal role in the regulation of non-small cell lung carcinoma (NSCLC). The present study aimed to investigate the antitumor effects of 7-difluoromethoxyl-5,4'-di-n-octylygenistein (DFOG), a novel synthetic genistein derivative, on NSCLC, and to elucidate its molecular mechanism. The research focused on whether DFOG inhibited self-renewal and tumor growth in NSCLC by modulating the miR-152-3p/STAT3 signaling pathway. Reverse transcription-quantitative PCR and western blot analyses were employed to assess miR-152-3p expression and phosphorylated-STAT3 (p-STAT3) levels. The effects of DFOG on self-renewal and tumor growth were evaluated via sphere formation and clonogenic assays. Additionally, sphere-forming cells (SFCs) were enriched using a suspension culture method, and western blot analysis was conducted to examine stemness markers (CD133, CD44, Oct4 and Sox2). The results demonstrated that DFOG inhibited self-renewal and tumor growth in NSCLC. This effect was associated with increased miR-152-3p expression, decreased STAT3 mRNA levels and reduced p-STAT3 levels in NSCLC cells. Furthermore, inhibition or overexpression of STAT3 did not alter miR-152-3p expression but modulated the inhibitory effects of DFOG on self-renewal and tumor growth. These findings highlighted that DFOG suppressed self-renewal and tumor growth in SFCs derived from NSCLC by directly targeting STAT3 through the upregulation of miR-152-3p.

Correspondence to: Dr Jiansong Zhang, Department of Preclinical Medicine, Medical College, Hunan Normal University, 371 Tongzipo Road, Yuelu, Changsha, Hunan 410013, P.R. China
E-mail: 14928@hunnu.edu.cn

Dr Jianhui Xiao, Institute of Medicinal Biotechnology, Affiliated Hospital of Zunyi Medical University, 149 Dalian Road, Huichuan, Zunyi, Guizhou 563003, P.R. China
E-mail: jhxiao@zmc.edu.cn

Abbreviations: DFOG, 7-difluoromethoxyl-5,4'-di-n-octylygenistein; NSCLC, non-small cell lung carcinoma; p-STAT3, phosphorylated-STAT3

Key words: DFOG, NSCLC, microRNA-152-3p, STAT3, self-renewal, tumor growth

Introduction

Non-small cell lung carcinoma (NSCLC), responsible for >80% of all lung cancer cases, is the deadliest form of malignancy worldwide (1). Despite advancements in therapeutic strategies such as surgical resection, chemotherapy, radiotherapy, immunotherapy and combination therapies, each focusing primarily on symptom alleviation, the 5-year overall survival rate of NSCLC remains <20% (2). This is further complicated by the widespread occurrence of chemoresistance and the increased metastatic potential of the disease, which undermine the efficacy of conventional treatments (3). This challenge is, at least in part, attributable to the self-renewal properties of cancer stem cells (4), which are resistant to chemotherapy, rendering traditional treatments less effective. As such, there is an urgent need for innovative therapeutic approaches targeting NSCLC cancer stem cells. Research has intensified efforts to understand self-renewal and tumor growth mechanisms, aiming to identify novel therapeutic targets or develop innovative curative interventions for various cancer types, including NSCLC (4-6). Studies have identified a small subset of tumor cells that, derived from bulk tumors, possess self-renewal and tumor-initiating abilities (7-9). These cells are typically enriched using cell surface markers (CD133, CD44, Sox2 and Oct4) or sphere formation assays in suspension culture (4,5,8,10,11). Notably, the sphere culture assay has proven effective in enriching sphere-forming cells (SFCs) from NSCLC cell lines, and SFCs exhibit stronger self-renewal potential (12,13). There is a critical need to develop effective therapeutic strategies, particularly novel targeted drugs aimed

at directly addressing cancer cell self-renewal and tumor growth in NSCLC.

Genistein, an isoflavone found abundantly in soybeans and related products, has exhibited anticancer properties across various malignancies such as retinoblastoma, laryngeal cancer and colorectal cancer (14-16). 7-difluoromethoxyl-5,4'-di-n-octylgenistein (DFOG), a new genistein analog synthesized independently by the Department of Pharmacy, Hunan Normal University (Changsha, China), has been shown to induce apoptosis in ovarian cancer cells, and to inhibit their self-renewal and carcinogenesis (17,18). Despite these promising findings, the exact mechanism through which DFOG suppresses self-renewal and tumor growth in NSCLC cells remains to be fully elucidated.

MicroRNAs (miRNAs/miRs) are evolutionarily conserved, endogenous small noncoding RNAs, typically 19-23 nucleotides in length (19). Despite lacking protein-coding potential, they regulate a wide array of genes post-transcriptionally through complementary binding to mRNAs (20). These molecules are critical in processes such as apoptosis, differentiation, proliferation and metabolism, making them central to cancer development and stemness in cancer cells (21). One such miRNA, miR-152, has been identified as a tumor suppressor and is linked to malignant phenotypes of various types of cancer such as colon cancer, breast cancer, prostate cancer and ovarian cancer (22-25). A recent study has demonstrated that miR-152-3p is involved in the self-renewal and tumor growth of non-small cell lung cancer (26). Additionally, miR-152-3p is associated with tumor invasion, metastasis, drug resistance and proliferation (27,28). However, whether DFOG can inhibit the self-renewal and tumor growth of NSCLC by regulating miR-152-3p remains to be determined.

Persistent activation of STAT3 impacts gene regulation, thereby influencing self-renewal, migration and invasion in cancer cells (29,30). The miR-152/STAT3 axis is associated with poor prognosis in epithelial ovarian cancer (31). A previous study using JSI-124, a specific STAT3 inhibitor, suggested that suppressing STAT3 activation can diminish stem cell-like properties in hepatocellular carcinoma cells (32). However, it remains unclear whether miR-152-3p-mediated STAT3 inactivation can effectively reduce the self-renewal and tumor growth of SFCs derived from NSCLC. Therefore, the present study aimed to examine the hypothesis that reinstating miR-152-3p expression to suppress STAT3 can synergistically enhance the inhibitory effects of DFOG on self-renewal and tumor growth in SFCs derived from NSCLC.

Materials and methods

Cells and sphere cultures. The NCI-H460 and NCI-A549 human NSCLC cell lines were obtained from Shanghai Zhong Qiao Xin Zhou Biotechnology Co., Ltd., and Procell Life Science & Technology Co., Ltd., respectively, while the BEP2D human bronchial epithelial cell line was sourced from Otwo Biotech. All cell lines were authenticated through short tandem repeat profiling and mycoplasma testing. The cells were cultured in DMEM (Gibco; Thermo Fisher Scientific, Inc.) supplemented with 10% FBS (Gibco; Thermo Fisher Scientific, Inc.), penicillin (100 U/ml) and streptomycin (100 μg/ml). All cells were maintained in a 5% CO_2 incubator at 37˚C. The STAT3 inhibitor S3I 201 (97%; cat. no. ab146606; Abcam) was stored at room temperature, and the cells were treated with S3I 201 (10 μM) at 37˚C for 24 h before subsequent experiments.

To study sphere formation, H460 and A549 cells were cultured in stem-cell culture medium at a density of 5,000 cells per well in ultra-low attachment 6-well plates until spheres containing >20 cells formed (12,13). Stem-cell culture medium (DMEM/F12; Gibco; Thermo Fisher Scientific, Inc.), supplemented with 2% B27, 1% penicillin/streptomycin, basic fibroblast growth factor (20 ng/ml), epidermal growth factor (20 ng/ml) and insulin (4 μg/ml), was used. The inhibitory effects of DFOG on sphere formation were assessed by incubating SFCs derived from H460 and A549 cells with varying concentrations of DFOG (1, 5 and 10 μM) at 37˚C for 72 h. Subsequently, the cells were reseeded at a density of 1,000 cells per well in ultra-low attachment 24-well plates and cultured until spheres reformed in the absence of DFOG. Subsequently, the number and status of spheres were evaluated manually under a light microscope (Leica Microsystems GmbH). The sphere formation rate was calculated using the following formula: Number of spheres/number of cells seeded x100%. Experiments were performed in triplicate.

Cell viability assessment. Cell viability was assessed using the Cell Counting Kit-8 (CCK-8) assay (Dojindo Laboratories, Inc.). Single-cell suspensions were seeded at 1,000 cells per well in 96-well plates for 24 h and treated with varying concentrations of DFOG (1, 5 and 10 μM) at 37˚C. After 72 h, the cells were incubated with 10 μl CCK-8 solution per well for 2 h, and the optical density (OD_{450}) was measured using a microplate reader (BioTek; Agilent Technologies, Inc.).

Reverse transcription-quantitative PCR (RT-qPCR). The Superscript IV RT kit and SYBR Green fluorophore were purchased from Thermo Fisher Scientific, Inc. The RT reaction conditions were incubation at 37˚C for 5 min, 50˚C for 15 min and 75˚C for 5 min. Total RNA was extracted from H460 cells, A549 cells or SFCs ($1x10^5$ cells) using TRIzol® reagent (Thermo Fisher Scientific, Inc.) according to the manufacturer's protocol. For RNA extraction from tissue samples, grinding using a tissue homogenizer (Beyotime Institute of Biotechnology) was first performed. cDNA synthesis was conducted according to the supplier's instructions (Thermo Fisher Scientific, Inc.). The $2^{-\Delta\Delta Cq}$ method (33) was used for qPCR, with U6 as the internal control for miR-152 and GAPDH as the internal control for STAT3. To identify candidate miRNAs affected by DFOG treatment, H460 cells, A549 cells or SFCs were treated with DFOG (5 μM) at 37˚C for 24 h, followed by total RNA extraction and cDNA synthesis. PCR amplification was performed using specific primers (Table I), with the following thermocycling conditions: 95˚C for 10 min, followed by 40 cycles of 95˚C for 30 sec, 55˚C for 30 sec and 70˚C for 30 sec. For miRNA quantification, 2 μg total miRNA was transcribed and amplified using the All-in-One™ miRNA qRT-PCR Detection Kit (Applied Biosystems; Thermo Fisher Scientific, Inc.) and the TaqMan MicroRNA Assay (GeneCopoeia, Inc.), with U6 (Sangon Biotech Co., Ltd.) as the reference gene. Data analysis was conducted using the $2^{-\Delta\Delta Cq}$ method. All experiments were conducted in triplicate independently.

Table I. Primer sequences for reverse transcription-quantitative PCR.

Gene name	Primer sequence (5'-3')
U6	F: CTCGCTTCGGCAGCACA
	R: AACGCTTCACGAATTTGCGT
STAT3	F: GGGAGAGAGTTACAGGTTGGACAT
	R: AGACGCCATTACAAGTGCCA
GAPDH	F: CGGAGTCAACGGATTTGGTCGTAT
	R: ATCCTTCTCCATGGTGGTGAAGAC
miR-671-5p	F: AGGAAGCCCTGGAGGGGC
	R: CAGTGCAGGGTCCGAGGTAT
miR-148a-3p	F: TCAGTGCACTACAGAACTTTGT
	R: AGTGCAGGGTCCGAGGTAT
miR-340-5p	F: TTATAAAGCAATGAGACTGATT
	R: AGTGCAGGGTCCGAGGTATT
miR-342-3p	F: TCTCACACAGAAATCGCACCC
	R: AGTGCAGGGTCCGAGGTAT
miR-34a-5p	F: TGGCAGTGTCTTAGCTGGTTGT
	R: AGTGCAGGGTCCGAGGTATT
miR-152-3p	F: TCAGTGCATGACAGAACTTGG
	R: TGCAGGGTCCGAGGTAT

AGTGCAGGGTCCGAGGTAT is a universal reverse primer. F, forward; miR, microRNA; R, reverse.

Table II. Maximum volume of the xenograft (mm^3) in each mouse across all experimental groups.

DFOG (0 mg/kg)	DFOG (10 mg/kg)	DFOG (50 mg/kg)
953.06	408.32	166.08
884.01	367.26	105.36
877.36	316.19	115.17
896.21	402.42	62.97
806.09	309.19	88.68
931.01	207.37	60.69

DFOG, 7-difluoromethoxyl-5,4'-di-n-octylygenistein.

Table III. Maximum diameter measured of the xenograft (mm) in each mouse across all experimental groups.

DFOG (0 mg/kg)	DFOG (10 mg/kg)	DFOG (50 mg/kg)
14.56	11.23	6.32
13.09	10.21	5.21
13.32	9.68	5.69
12.25	8.99	4.62
14.32	8.32	5.17
14.87	7.96	4.16

DFOG, 7-difluoromethoxyl-5,4'-di-n-octylygenistein.

Clonogenic assay. For the colony formation assay, a bottom agar layer was prepared by mixing 1.2% agarose (Invitrogen; Thermo Fisher Scientific, Inc.) with DMEM in equal proportions, and 500 μl of this mixture was added to each well of a 24-well plate. The top agar layer was prepared by mixing H460 cells, A549 cells or SFCs (1,000 cells) with 0.7% agarose and 500 μl of 20% FBS-supplemented DMEM. After 12 h of cell seeding, different concentrations of DFOG (1, 5 and 10 μM) were added according to the needs of each group. The drug was continuously administered at 37˚C until the end of the experiment. Images of colony formation were captured under a light microscope (Leica Microsystems GmbH) and colonies were counted manually. More than 20 cells were defined as a colony. The cells were incubated for 14 days at 37˚C, and colonies were counted to calculate the colony formation rate per 1,000 cells based on triplicate experiments.

Immunoblot assay. The RIPA protein extraction kit was purchased from Thermo Fisher Scientific, Inc. BCA was used to quantitatively determine the protein concentration. Each lane was loaded with 20 μg of protein. The gel concentration used was 10%. After electrophoresis, protein was transferred to a PVDF membrane. Blocking was performed using 5% skimmed milk at 37˚C for 1 h. Membranes were incubated with the primary antibody at 4˚C for 6 h, and membranes were incubated with the horseradish peroxidase-conjugated IgG secondary antibody (1:1,000 dilution; cat. no. RGAR011; Proteintech Group, Inc.) at room temperature for 1 h. Antibodies against α-tubulin (1:1,000 dilution; cat. no. 2125; Cell Signaling Technology, Inc.), STAT3 (1:1,000 dilution; cat. no. 12640; Cell Signaling Technology, Inc.), phosphorylated-STAT3 (p-STAT3; 1:2,000 dilution; cat. no. 9145; Cell Signaling Technology, Inc.), CD133 (1:1,000 dilution; cat. no. 64326; Cell Signaling Technology, Inc.), CD44 (1:1,000 dilution; cat. no. 37259; Cell Signaling Technology, Inc.), Oct4 (1:1,000 dilution; cat. no. 2890; Cell Signaling Technology, Inc.) and Sox2 (1:1,000 dilution; cat. no. 3579; Cell Signaling Technology, Inc.) were used as previously described (12). Finally, the chemiluminescent substrate (ECL) was purchased from Beyotime Institute of Biotechnology, and ImageJ 1.37 (National Institutes of Health) was used for gray-scale analysis.

miRNA transfection. MicrON™ miR-152-3p mimic (5'-UCAGUGCAUGACAGAACUUGG-3') and micrOFF™ miR-152-3p inhibitor (5'-CCAAGUUCUGUCAUGCACUGA-3'), miR-152-3p mimic negative control (5'-UUGUACUACACAAAAGUACUG-3') and miR-152-3p inhibitor negative control (5'-GGAACUUAGCCACUGUGAAUU-3'), were purchased from Guangzhou RiboBio Co., Ltd., and transfected into SFCs using transfection reagent iboFECT™ CP (Guangzhou RiboBio Co., Ltd.) at a concentration of 50 nM, according to the manufacturer's instructions. The small RNA complexes were incubated with cells for 2 h before the medium was replaced, then the culture was continued at 37˚C for 48 h, and cells were used for subsequent experiments.

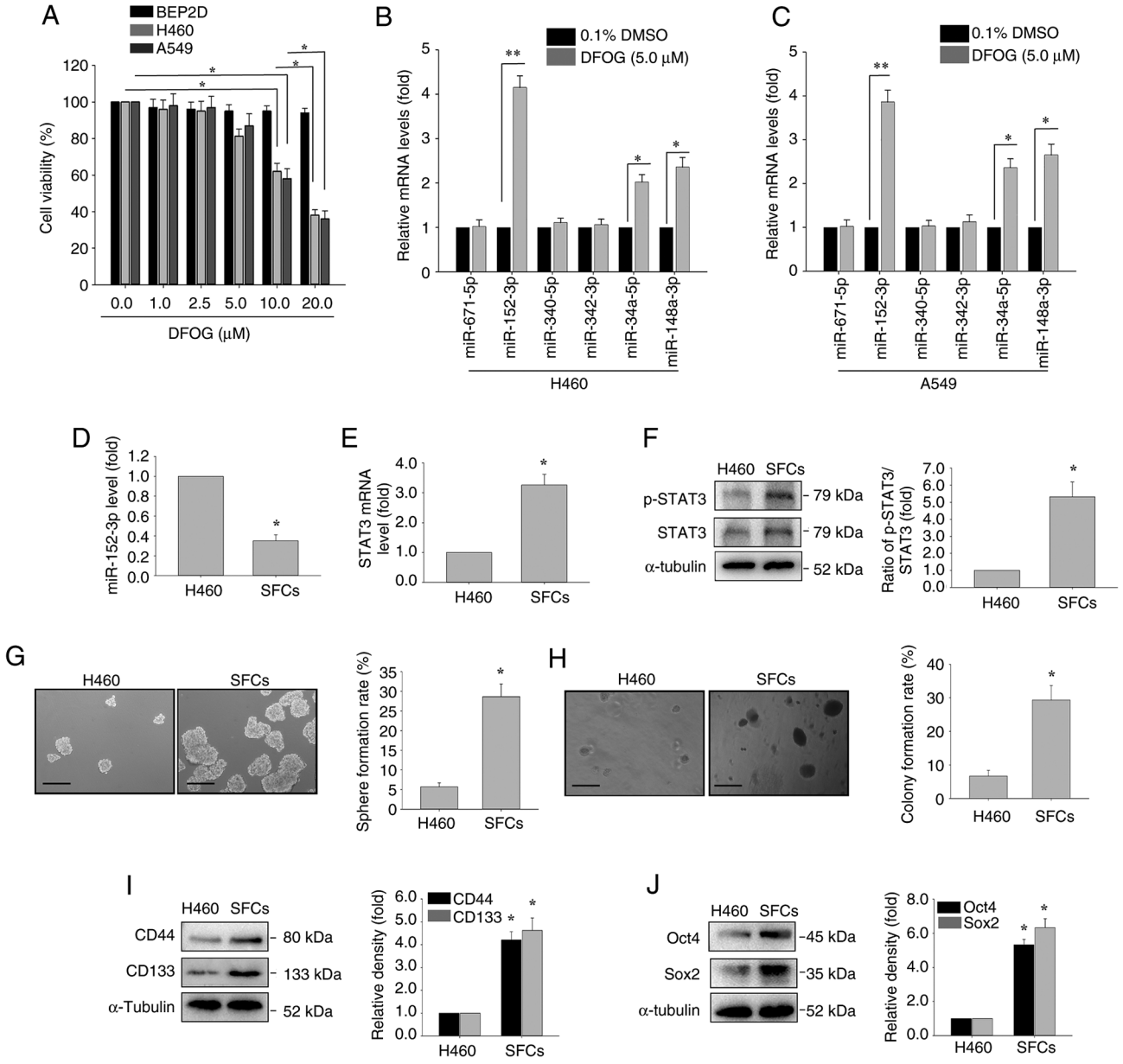

Figure 1. mRNA expression analysis by RT-qPCR, and assessment of self-renewal and tumor growth in H460-derived SFCs. (A) BEP2D, H460 and A549 cells were treated with DFOG (0-20 μM) for 48 h, and cell viability was assessed using a Cell Counting Kit-8 assay. H460 and A549 cells were treated with DFOG (5 μM) for 24 h. RT-qPCR was used to evaluate the effects of DFOG (5 μM) on tumor-suppressive miRNAs, including miR-671-5p, miR-148a-3p, miR-340-5p, miR-342-3p, miR-34a-5p and miR-152-3p in (B) H460 and (C) A549 cells. (D) Comparison of miR-152-3p expression between H460 cells and H460-derived SFCs. (E) STAT3 mRNA levels and (F) p-STAT3 protein levels. Rates of (G) sphere formation and (H) colony formation (scale bar, 100 μm). Western blot analysis of (I) CD44 and CD133 expression, as well as (J) Oct4 and Sox2 expression. *P<0.05, **P<0.01 (n=3). DFOG, 7-difluoromethoxyl-5,4'-di-n-octylygenistein; miR/miRNA, microRNA; p-, phosphorylated; RT-qPCR, reverse transcription-quantitative PCR; SFC, sphere-forming cell.

Luciferase reporter assay. The binding sites of miR-152-3p and STAT3 were predicted using RNAhybrid (http://bibiserv.techfak.uni-bielefeld.de/rnahybrid). For the luciferase reporter assays, SFCs were co-transfected with miR-152-3p or miR-control and the pGL3 luciferase vector (Guangzhou RiboBio Co., Ltd.) containing the firefly luciferase reporter, along with the wild-type (WT) or mutant (MUT) 3'-untranslated region (UTR) sequence of STAT3. After 48 h, luciferase activity was measured using a luciferase assay kit (Promega Corporation), and normalized to *Renilla* luciferase activity in triplicate experiments.

Plasmid transfection. Transfection was performed using 10 μg nucleic acid with a concentration of 1 μg/μl at 37˚C for 48 h, and subsequent experiments were performed 48 h after transfection. For STAT3 overexpression, cells were transfected with pcDNA3.1-Control or pcDNA3.1-STAT3 plasmids obtained from Invitrogen; Thermo Fisher Scientific, Inc., using Lipofectamine™ 2000 (Invitrogen; Thermo Fisher Scientific, Inc.) in Opti-MEM (Gibco; Thermo Fisher Scientific, Inc.), according to the manufacturer's guidelines.

In vivo therapeutic effects in nude mice. A total of 18 female pathogen-free nude BALB/c mice (aged 4-5 weeks; weight, 18-22 g) were sourced from GemPharmatech Co., Ltd., and housed in a specific pathogen-free facility [SYXK (Xiang) 2020-0012] under a standard 12-h light/12-h dark cycle,

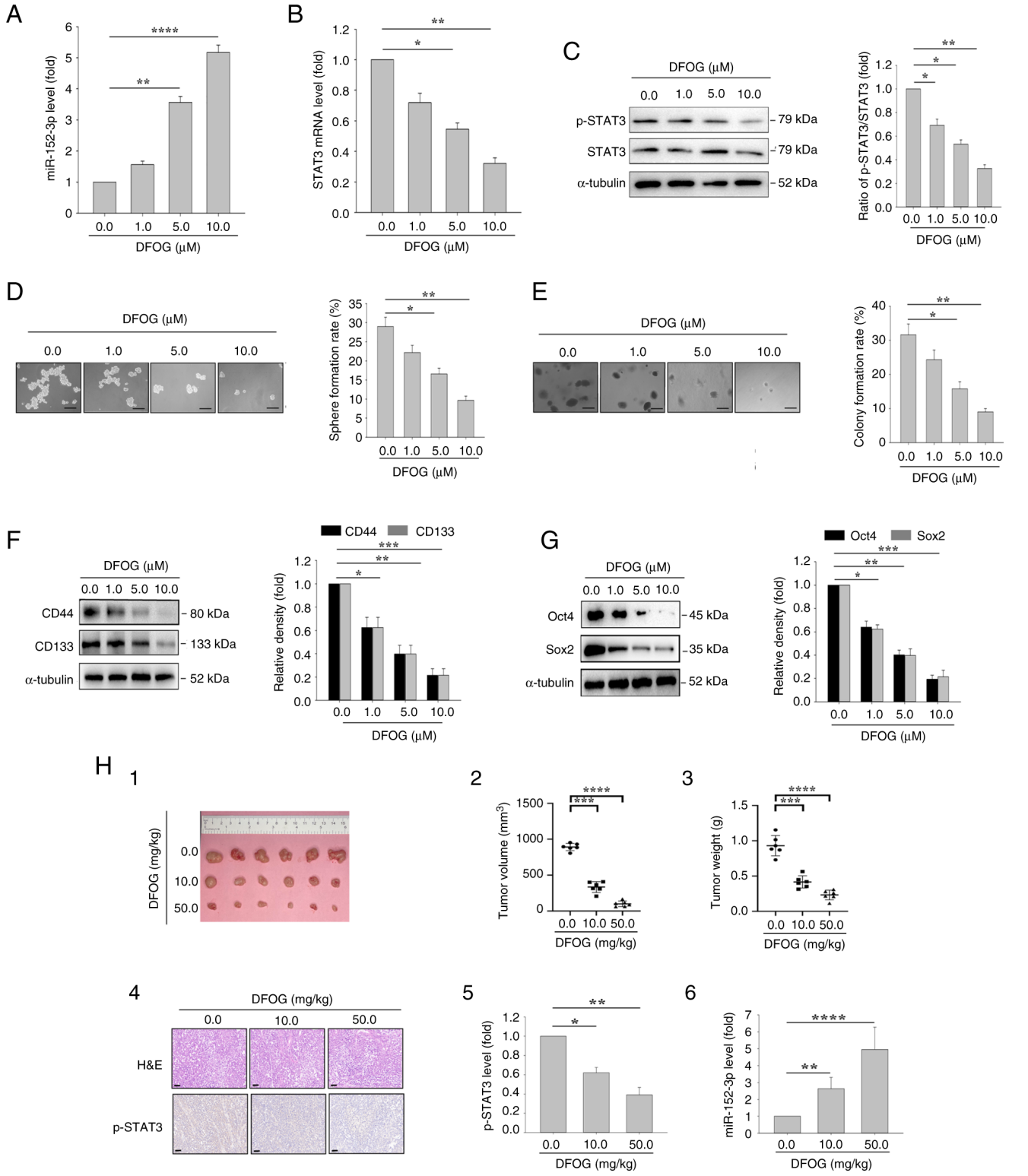

Figure 2. DFOG induces miR-152-3p expression, and inhibits self-renewal and tumor growth in H460-derived SFCs. At the indicated concentrations, DFOG (A) upregulated miR-152-3p expression, and (B) decreased STAT3 mRNA expression and (C) p-STAT3 protein levels in H460-derived SFCs. (D) Sphere formation and (E) colony formation were reduced (scale bar, 100 μm). Western blot analysis showed downregulation of (F) CD44 and CD133 expression, as well as (G) Oct4 and Sox2 expression. *P<0.05, **P<0.01,***P<0.001, ****P<0.0001 (n=3). (H) (1) Images of tumor tissue; (2) volume quantification; (3) weight quantification; (4) H&E staining and immunohistochemical staining using an anti-p-STAT3 antibody (scale bar, 50 μm). (5) Quantification of p-STAT3 protein levels and (6) miR-152-3p levels in xenograft tumors of nude mice bearing H460-derived SFCs treated with DFOG at the indicated doses. *P<0.05, **P<0.01, ***P<0.001, ****P<0.0001. DFOG, 7-difluoromethoxyl-5,4'-di-n-octylygenistein; miR, microRNA; p-, phosphorylated; SFC, sphere-forming cell.

at 20-26˚C, with an atmospheric pressure of 20-50 Pa and a relative humidity of 40-70%, and *ad libitum* access to regular mouse chow and water. The site of cell injection was the armpit of the upper limb. When the tumor grew to ~100 cm^3, the mouse was treated with drug treatment for 21 days. The time interval between the injection of cells and

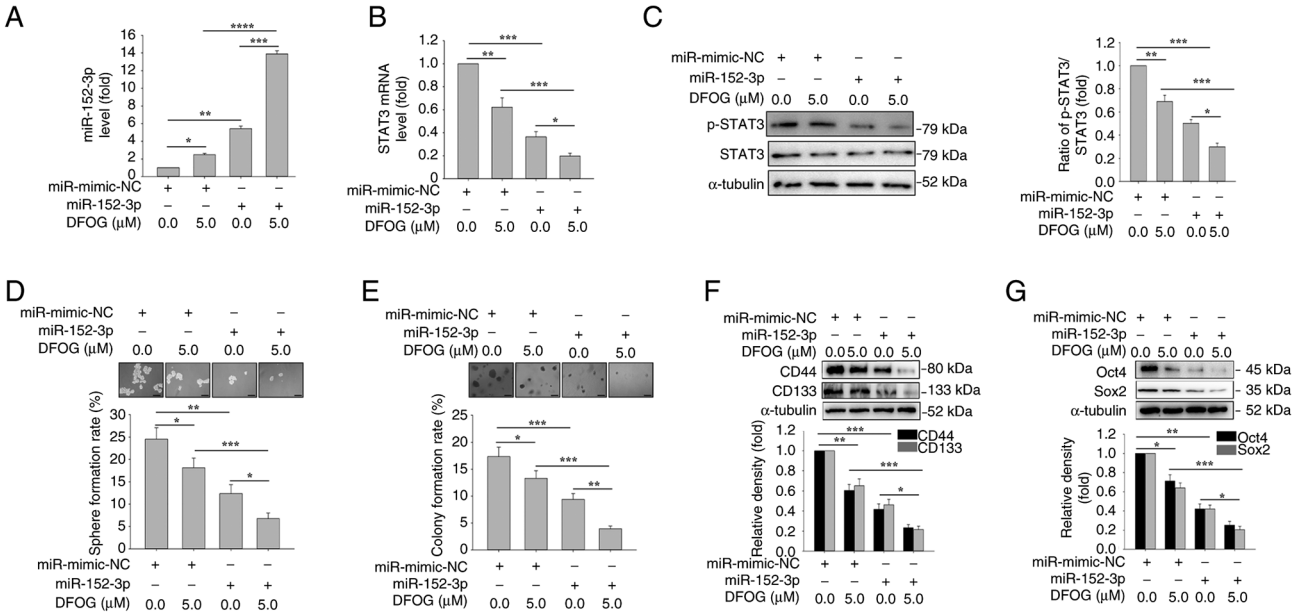

Figure 3. miR-152-3p mimic enhances DFOG-induced downregulation of p-STAT3 levels and inhibits self-renewal in H460-derived SFCs. Expression levels of (A) miR-152-3p and (B) STAT3 mRNA, and (C) p-STAT3 protein levels. (D) Spheres and (E) colonies formed were quantified (scale bar, 100 μm). Western blot analysis of (F) CD44 and CD133, as well as (G) Oct4 and Sox2 expression in H460-derived SFCs transfected with miR-152-3p mimic and/or treated with DFOG (5 μM). *P<0.05, **P<0.01, ***P<0.001 and ****P<0.0001 (n=3). DFOG, 7-difluoromethoxyl-5,4'-di-n-octylygenistein; miR, microRNA; NC, negative control; p-, phosphorylated; SFC, sphere-forming cell.

the end of the experiment was 6 weeks, and tumor volume was detected every 2 days until the end of the experiment. The ethical approval (approval no. D2023045) was granted by the Ethics Committee of Hunan Normal University (Changsha, China).

To evaluate the effects of DFOG in the xenograft mouse model, 1x10^6 SFCs were suspended in PBS and mixed with 100% Matrigel at a 1:1 ratio (BD Biosciences). A 100 μl mixture was subcutaneously injected into each mouse. When the xenograft volume reached ~100 mm^3, mice in the control group received 200 μl of 2% DMSO every 2 days, while those in the experimental groups were orally administered DFOG (10 and 50 mg/kg) for 3 weeks every 2 days. Each group consisted of 6 mice. Tumor volume was calculated using the following formula: V (mm^3)=(L x W^2)/2, where L is the longest diameter and W is the shortest diameter of the xenograft, measured using a Vernier caliper. At the end of the experiment, xenograft-bearing mice were euthanized using CO_2 asphyxiation (CO_2 replacement rate of 30%), and the xenografts were collected, weighed, and snap-frozen in liquid nitrogen, and tumor tissues were fixed in 4% paraformaldehyde for subsequent H&E staining and immunohistochemistry. Tumor tissues for qPCR analysis were preserved in RNAlater.

For H&E staining, tumor tissues were fixed in 4% paraformaldehyde at 4˚C for 24 h, and the slice thickness was 4 μm. Hematoxylin staining was performed for 5 min, followed by eosin staining for 1 min, and these were performed at 25˚C. Staining was observed under a light microscope (Leica Microsystems GmbH).

Immunohistochemical staining. Tumor tissues were fixed in 4% paraformaldehyde at 4˚C for 24 h. Tissue sections (thickness, 4 μm) from paraffin-embedded and fixed samples were subjected to deparaffinization in citrate buffer. Sections were heated in an oven at 90˚C for 20 min, followed by a series of ethanol washes (anhydrous ethanol, 95, 85 and 75% ethanol). Subsequently, the slices underwent three consecutive washes with PBS. After blocking endogenous peroxidase activity with 3% H_2O_2 and nonspecific binding with 5% goat serum (Beyotime Institute of Biotechnology) for 15 min at 25˚C, the sections were incubated overnight at 4˚C with the primary antibody against p-STAT3 (1:200 dilution; cat. no. 9145; Cell Signaling Technology, Inc.). As a negative control, PBS was used in place of the primary antibody. The sections were then incubated with horseradish peroxidase-conjugated anti-rabbit IgG antibodies (1:500 dilution; cat. no. RGAR011; Proteintech Group, Inc.) for 20 min at 25˚C. Staining was developed using the 3,3'diaminobenzidine substrate (Fuzhou Maixin Biotechnology Development Co., Ltd.). The results were observed and images were captured under a light microscope (Leica Microsystems GmbH). The signal intensity was evaluated as previously described (34), and semi-quantitatively analyzed using ImageJ 1.37.

Statistical analysis. All statistical analyses were performed using GraphPad Prism Software 9 (Dotmatics). Data are presented as the mean ± SD. Comparisons between groups were performed using one-way analysis of variance with Tukey's post hoc test or an unpaired Student's t-test. For *in vitro* analyses, experiments were performed in triplicate. P<0.05 was considered to indicate a statistically significant difference.

Results

DFOG small-scale miRNAs efficacy screen, and analysis of self-renewal-related stemness of H460-derived SFCs.

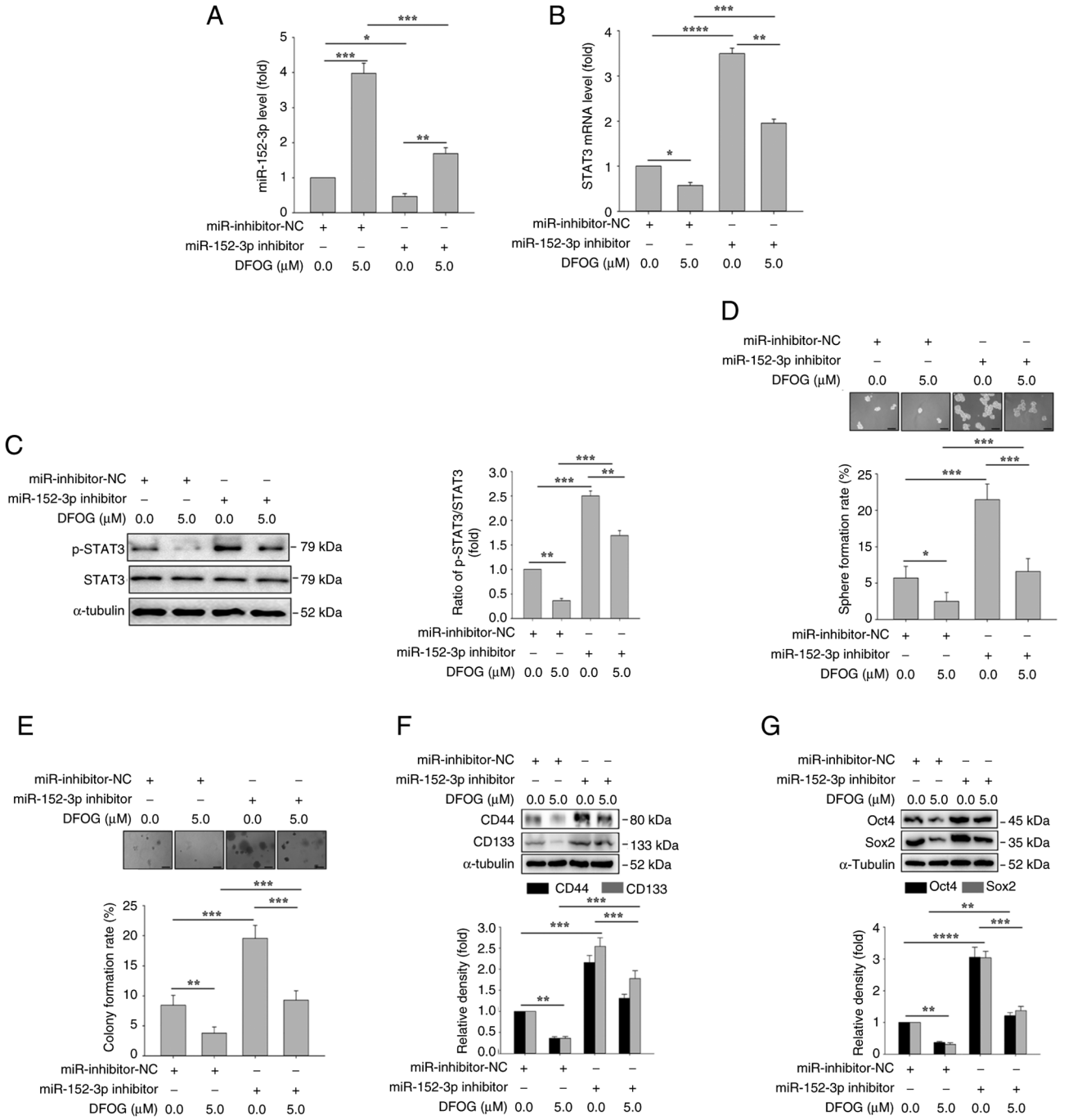

Figure 4. miR-152-3p inhibitor antagonizes DFOG-induced suppression of p-STAT3 levels and self-renewal in H460-derived SFCs. Expression levels of (A) miR-152-3p and (B) STAT3 mRNA, and (C) p-STAT3 protein levels. (D) Spheres and (E) colonies formed were quantified (scale bar, 100 μm). Western blot analysis of (F) CD44 and CD133, as well as (G) Oct4 and Sox2 expression in H460-derived SFCs transfected with miR-152-3p inhibitor and/or treated with DFOG (5 μM). *P<0.05, **P<0.01, ***P<0.001 and ****P<0.0001 (n=3). DFOG, 7-difluoromethoxyl-5,4'-di-n-octylygenistein; miR, microRNA; NC, negative control; p-, phosphorylated; SFC, sphere-forming cell.

The effect of DFOG on cell viability was assessed in BEP2D, H460 and A549 cell lines using the CCK-8 assay, following treatment at various concentrations. A reduction in cell viability was observed in H460 and A549 cells compared with the control group (0 μM), yielding an IC_{50} of ~10 μM (Fig. 1A). Noncytotoxic concentrations of DFOG (1, 5 and 10 μM) were selected for subsequent experiments.

Natural phytochemicals have been reported to modulate miRNA-mediated suppression of stemness characteristics in hepatocellular carcinoma cells (34). Therefore, it was detected whether tumor suppressor miRNAs in NSCLC cells, including miR-671-5p (31), miR-148a-3p (35), miR-340-5p (36), miR-342-3p (37), miR-34a-5p (38) and miR-152-3p (39), are regulated by DFOG (5 μM). DFOG treatment (5 μM) led to significant upregulation of miR-152-3p in both H460 and A549 cell lines, with the most notable increase among the tested miRNAs (Fig. 1B and C).

To examine the role of miR-152-3p and STAT3 expression in self-renewal and tumor growth in NSCLC, miR-152-3p

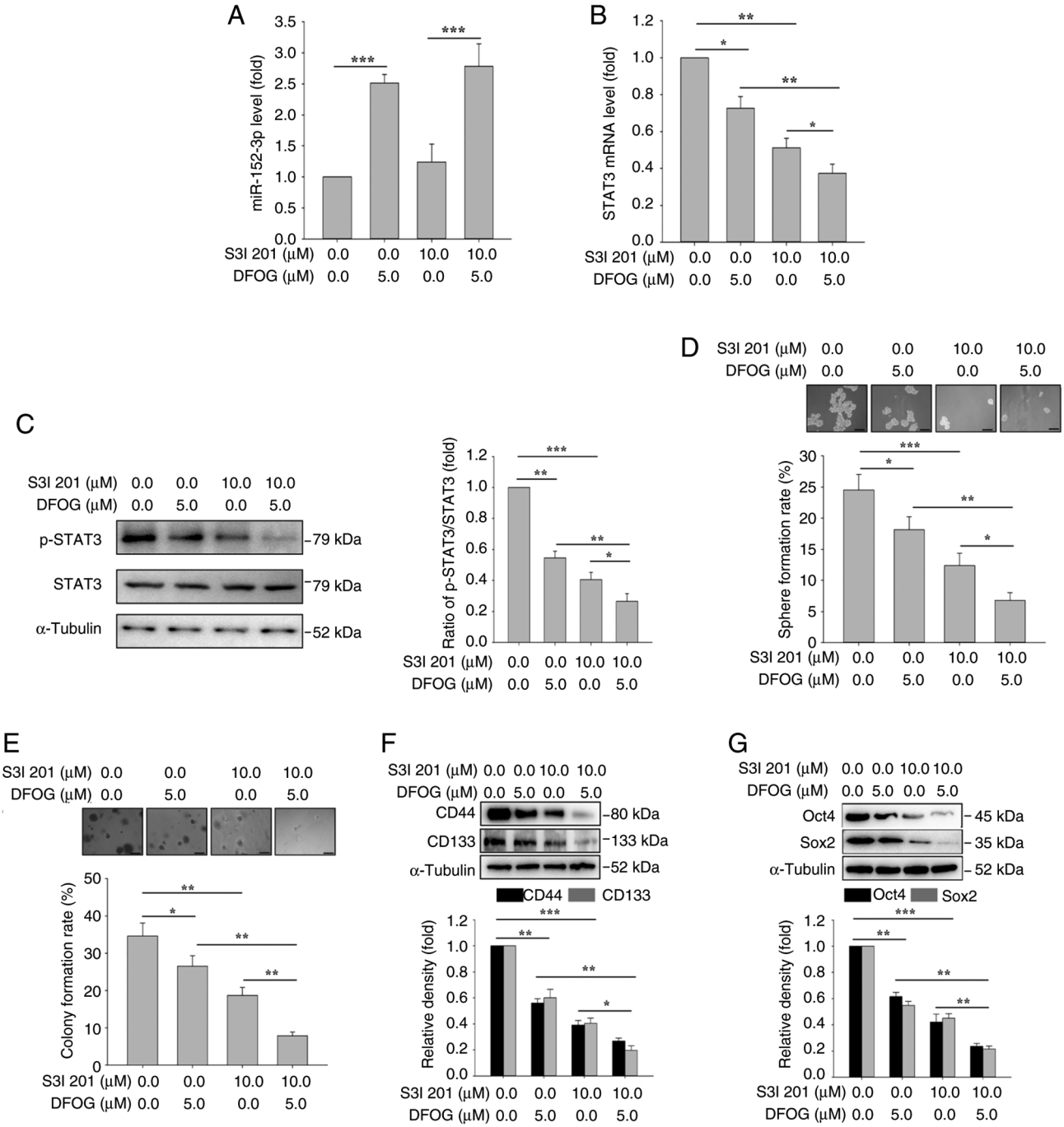

Figure 5. STAT3 inhibitor enhances DFOG-induced suppression of self-renewal in H460-derived SFCs. Expression levels of (A) miR-152-3p and (B) STAT3 mRNA, and (C) p-STAT3 protein levels are shown. (D) Spheres and (E) colonies formed were quantified (scale bar, 100 μm). Western blot analysis of (F) CD44 and CD133, as well as (G) Oct4 and Sox2 expression in H460-derived SFCs treated with S3I 201 (10 μM) and/or DFOG (5 μM). *P<0.05, **P<0.01 and ***P<0.001 (n=3). DFOG, 7-difluoromethoxyl-5,4'-di-n-octylygenistein; miR, microRNA; p-, phosphorylated; SFC, sphere-forming cell.

expression was compared between H460 cells and H460-derived SFCs. The results revealed lower miR-152-3p levels in SFCs compared with H460 cells (Fig. 1D). Additionally, SFCs exhibited elevated STAT3 mRNA expression and p-STAT3 levels (Fig. 1E and F).

The sphere formation and colony formation were significantly increased in H460-derived SFCs compared with H460 cells (Fig. 1G and H). Furthermore, the expression levels of stem cell-associated markers, including CD133, CD44, Oct4 and Sox2, were elevated in H460-derived SFCs compared with H460 cells (Fig. 1I and J).

DFOG inhibits self-renewal-related stemness possibly by upregulating miR-152-3p and inhibiting p-STAT3 in H460-derived SFCs. DFOG treatment at noncytotoxic concentrations (1, 5 and 10 μM) induced a dose-dependent increase in miR-152-3p expression in H460-derived SFCs (Fig. 2A). miR-152-3p has been recognized for its role in suppressing carcinogenesis by inhibiting carcinogenic transcription factors and signaling pathways in colon cancer, breast cancer, prostate cancer and ovarian cancer (22-25). Subsequently, the effects of DFOG on STAT3 mRNA expression and p-STAT3 protein levels were assessed using RT-qPCR and western blotting. DFOG treatment

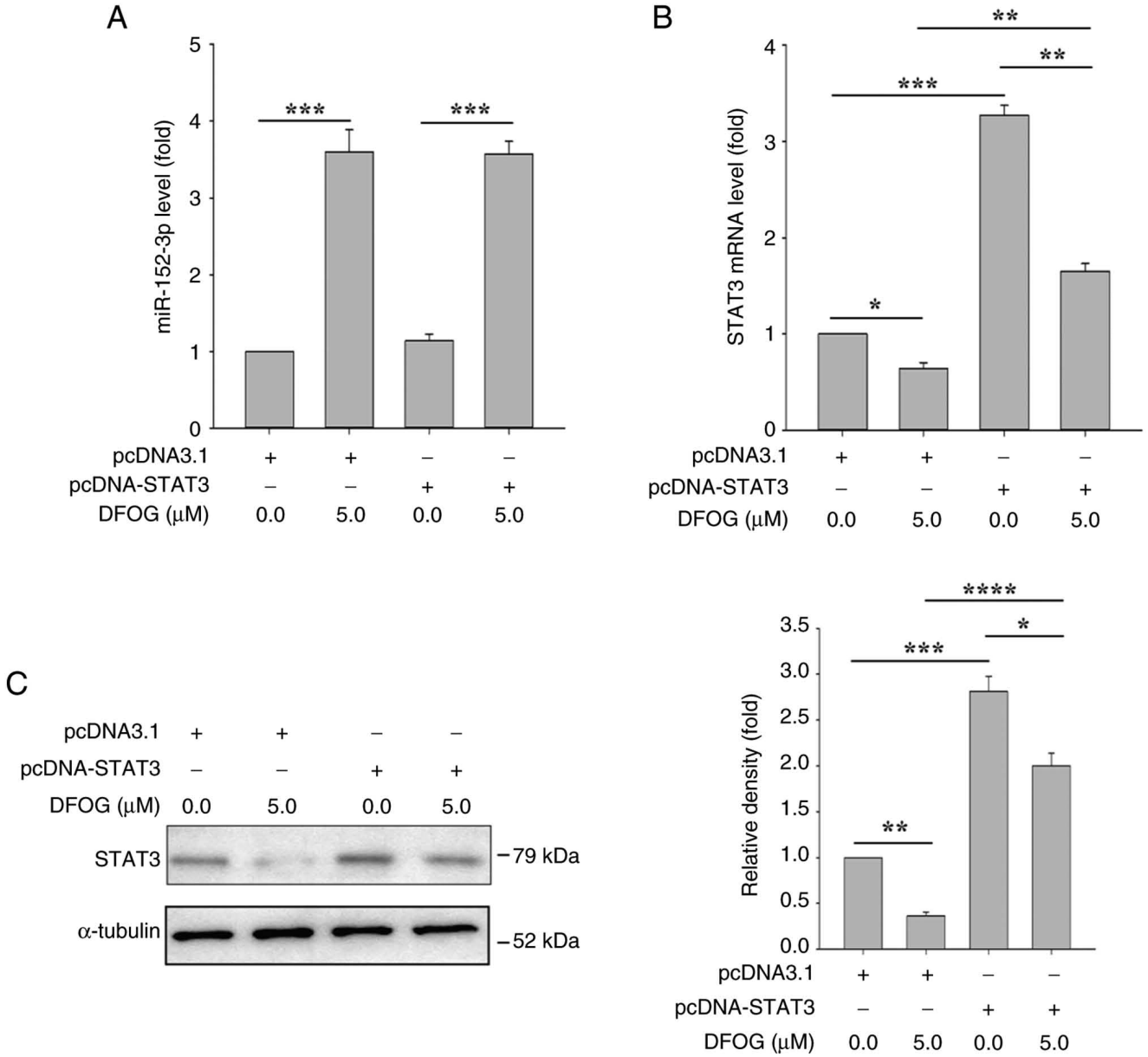

Figure 6. Effect of STAT3 overexpression and DFOG co-treatment on miR-152-3p expression. Expression levels of (A) miR-152-3p and (B) STAT3 mRNA, and (C) STAT3 protein levels in H460-derived sphere-forming cells transfected with pcDNA-STAT3 and/or treated with DFOG (5 μM). *P<0.05, **P<0.01, ***P<0.001 and ****P<0.0001 (n=3). DFOG, 7-difluoromethoxyl-5,4'-di-n-octylygenistein; miR, microRNA.

resulted in a decrease in STAT3 mRNA expression (Fig. 2B) and a significant reduction in p-STAT3 protein levels (Fig. 2C).

To evaluate the effect of DFOG on self-renewal and tumor growth in NSCLC, sphere formation and colony formation assays were performed. DFOG treatment led to reduced sphere (Fig. 2D) and colony (Fig. 2E) formation rates in H460-derived SFCs. Additionally, the protein levels of the stem cell markers CD133 and CD44 were significantly decreased (Fig. 2F). Consistent with these results, DFOG treatment substantially decreased the protein levels of Oct4 and Sox2 (Fig. 2G) in H460-derived SFCs.

For *in vivo* assessment, DFOG was orally administered to mice with H460-derived SFC xenograft tumors, with DMSO administered in the control group. The volumes of xenografts are shown in Table II and the maximum diameter is shown in Table III. As shown in Fig. 2H-1, -2 and -3, DFOG significantly suppressed the growth of xenograft tumors. Mechanistically, DFOG exerted a dual effect by reducing the p-STAT3 levels (Fig. 2H-4 and -5) and enhancing miR-152-3p expression (Fig. 2H-6). These results suggested that DFOG inhibited the self-renewal and tumor growth of H460-derived SFCs both *in vitro* and *in vivo*, likely through modulation of miR-152-3p and its target, STAT3.

miR-152-3p mimic increases DFOG-induced suppression of p-STAT3 and self-renewal. To further elucidate the role of miR-152-3p regulation in DFOG-mediated suppression of self-renewal, H460-derived SFCs were transfected with a miR-152-3p mimic. As shown in Fig. 3A, the miR-152-3p mimic, in combination with DFOG (5 μM), elevated miR-152-3p expression. Furthermore, both DFOG (5 μM) and the miR-152-3p mimic synergistically reduced STAT3

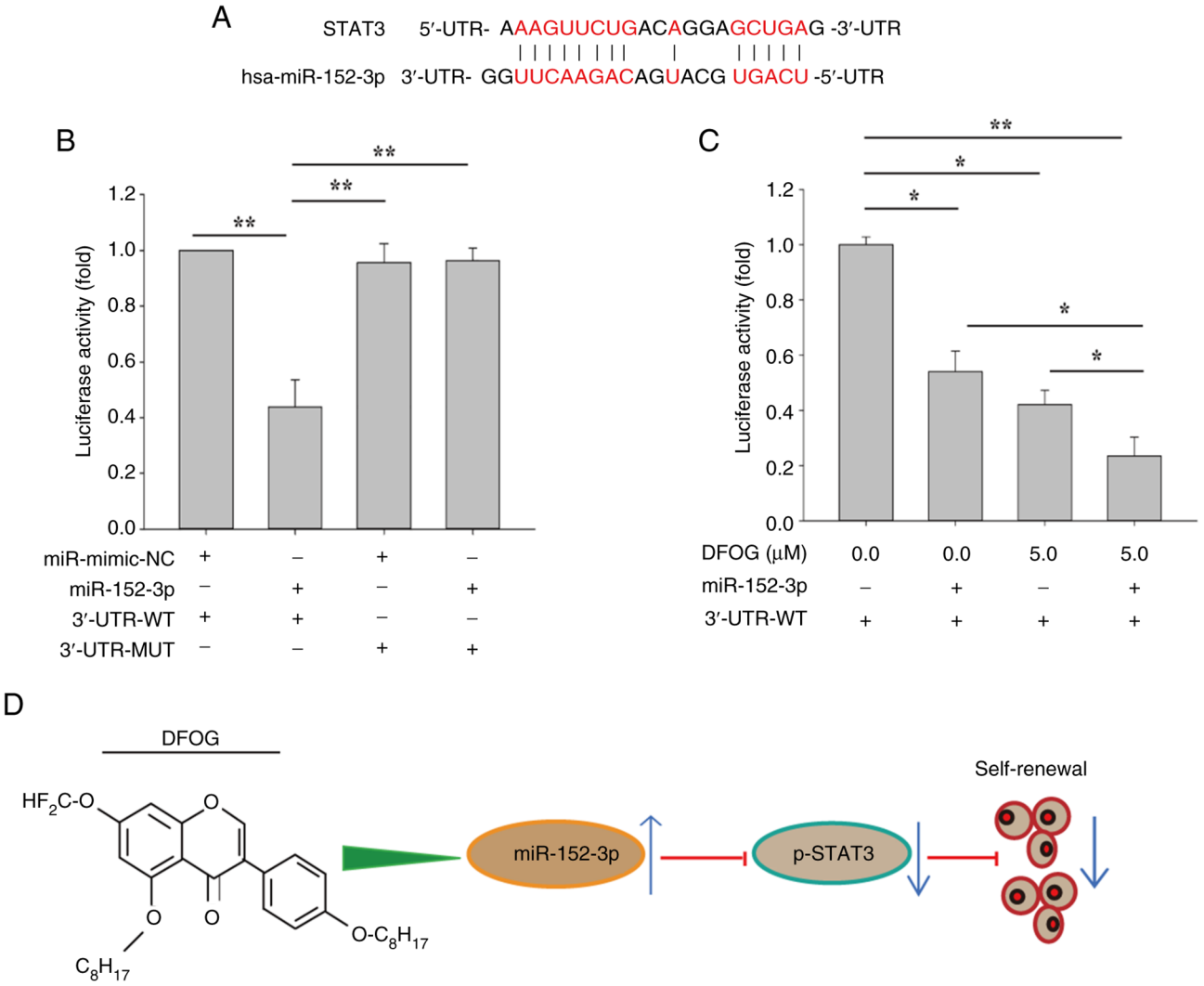

Figure 7. STAT3 is a direct target of miR-152-3p (https://bibiserv.cebitec.uni-bielefeld.de/rnahybrid). (A) Representation of the predicted miR-152-3p binding site in the 3'-UTR of STAT3 mRNA. (B) Luciferase activity of 3'-UTR-WT and 3'-UTR-MUT STAT3 3'-UTR reporters in H460 cells after transfection with the miR-152-3p mimic or miR-mimic-Cont. (C) Luciferase activity of 3'-UTR-WT STAT3 3'-UTR in H460 cells transfected with the miR-152-3p mimic and/or treated with DFOG (5 μM). *P<0.05, **P<0.01 (n=3). (D) Mechanism of action of DFOG regulating the miR-152-3p/STAT3 axis and suppressing self-renewal in non-small cell lung carcinoma. 3'-UTR, 3'-untranslated region; Cont, control; DFOG, 7-difluoromethoxyl-5,4'-di-n-octylygenistein; miR, microRNA; MUT, mutant; p-, phosphorylated; WT, wild-type.

mRNA levels and p-STAT3 protein levels (Fig. 3B and C). Notably, miR-152-3p overexpression enhanced the inhibitory effects of DFOG on self-renewal, leading to a reduction in sphere (Fig. 3D) and colony (Fig. 3E) formation rates compared with the control group (0 μM). The combined action of miR-152-3p and DFOG resulted in decreased expression of the stemness markers CD133 and CD44 (Fig. 3F), as well as the pluripotent factors Oct4 and Sox2 (Fig. 3G). These results suggested that DFOG elevated miR-152-3p expression, which in turn suppressed STAT3 transcription and activity, thereby inhibiting self-renewal in H460-derived SFCs.

miR-152-3p inhibitor antagonizes DFOG-induced suppression of p-STAT3 expression and self-renewal. To further validate the role of miR-152-3p regulation in DFOG-induced suppression of self-renewal, H460-derived SFCs were transfected with miR-152-3p inhibitor or miR-inhibitor-NC, followed by treatment with or without DFOG (5 μM). As shown in Fig. 4A, miR-152-3p inhibitor transfection effectively reversed the DFOG-induced increase in miR-152-3p expression. Additionally, miR-152-3p inhibitor counteracted the reduction in STAT3 mRNA expression and p-STAT3 protein levels induced by DFOG (Fig. 4B and C). Notably, miR-152-3p inhibitor mitigated the inhibitory effects of DFOG on self-renewal, as evidenced by an increase in sphere (Fig. 4D) and colony formation rates (Fig. 4E). miR-152-3p inhibitor transfection also increased the expression of the stemness-associated markers CD133 and CD44 (Fig. 4F), and the pluripotent factors Oct4 and Sox2 (Fig. 4G), reversing the suppressive effect of DFOG. These results suggested that inhibiting the expression of miR-152-3p could counteract the inhibition of p-STAT3 activity and self-renewal induced by DFOG treatment in H460-derived SFCs.

STAT3 inhibitor increases DFOG-induced self-renewal. To investigate whether the DFOG-induced suppression of self-renewal was linked to the regulation of STAT3 mRNA

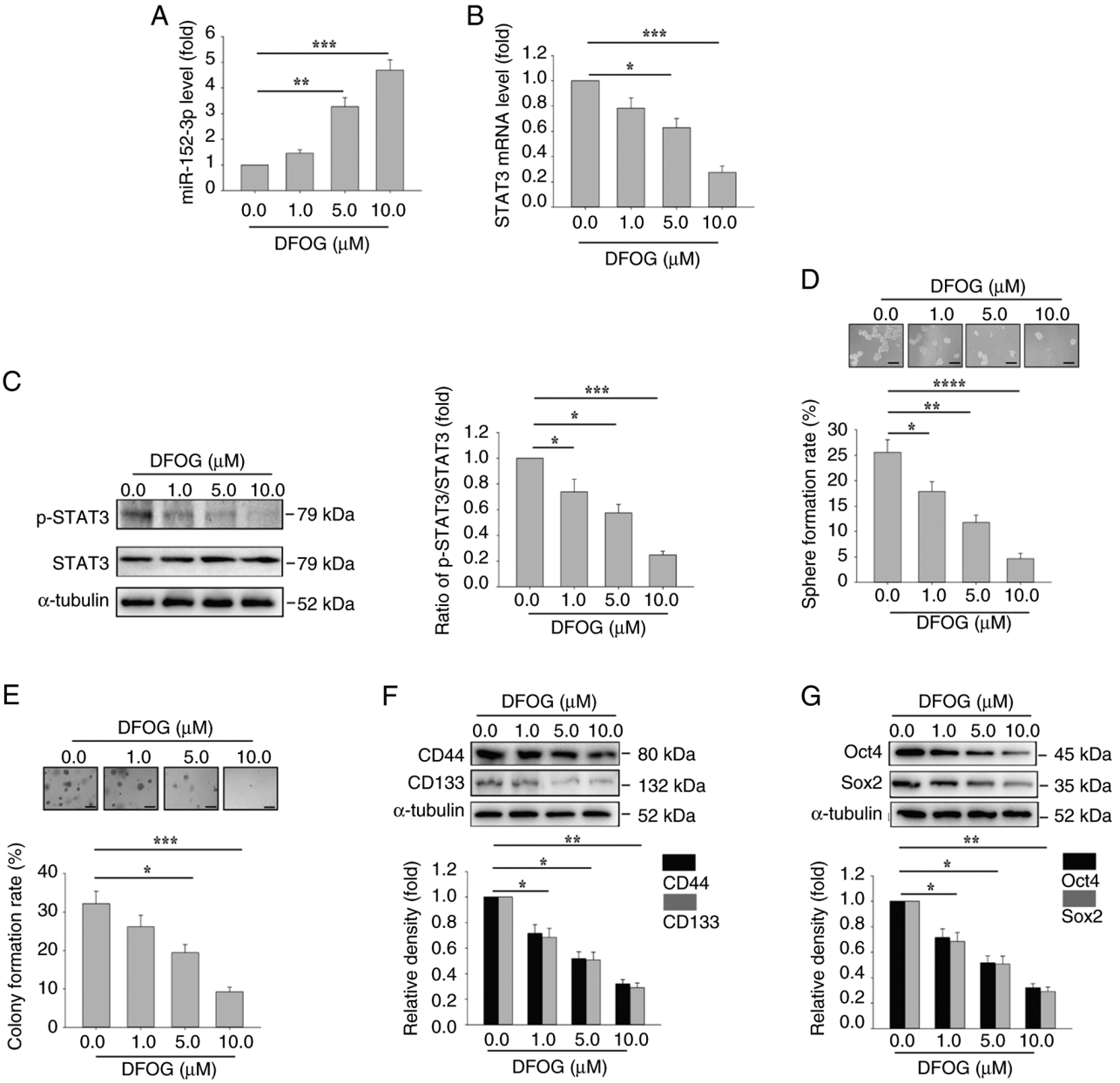

Figure 8. DFOG induces miR-152-3p expression, and inhibits STAT3 activation and self-renewal in A549-derived SFCs. At the indicated concentrations, DFOG (A) upregulated miR-152-3p expression, and decreased (B) STAT3 mRNA expression and (C) p-STAT3 protein levels in A549-derived SFCs. (D) Spheres and (E) colonies formed were quantified (scale bar, 100 μm). Western blot analysis of (F) CD44 and CD133, as well as (G) Oct4 and Sox2 expression in A549-derived SFCs. *P<0.05, **P<0.01, ***P<0.001 and ****P<0.0001 (n=3). DFOG, 7-difluoromethoxyl-5,4'-di-n-octylygenistein; miR, microRNA; p-, phosphorylated; SFC, sphere-forming cell.

expression and activity, H460-derived SFCs were treated with S3I 201, a specific STAT3 inhibitor. As shown in Fig. 5A, S3I 201 (10 μM) treatment did not affect the DFOG-induced elevation of miR-152-3p expression. However, as illustrated in Fig. 5B and C, S3I 201 (10 μM), in combination with DFOG (5 μM), effectively decreased STAT3 mRNA expression and p-STAT3 protein levels. Inhibition of STAT3 activity enhanced the suppressive effects of DFOG on self-renewal compared with S3I 201 (10 μM) or DFOG (5 μM) treatment alone, leading to a significant reduction in sphere (Fig. 5D) and colony (Fig. 5E) formation rates. Furthermore, the combination of S3I 201 and DFOG resulted in decreased protein levels of the stemness markers CD133 and CD44 (Fig. 5F), as well as the pluripotent factors Oct4 and Sox2 (Fig. 5G). These results highlighted that modulation of STAT3 mRNA expression and activity by DFOG contributed to the suppression of self-renewal in H460-derived SFCs.

STAT3 overexpression does not significantly affect miR-152-3p expression. To verify the upstream and downstream relationship between miR-152-3p and STAT3, H460-derived SFCs were transfected with STAT3 cDNA and pcDNA3.1, followed by treatment with or without DFOG (5 μM). As shown in Fig. 6A, transfection with STAT3 cDNA did not affect the miR-152-3p expression induced by DFOG. However, STAT3 cDNA transfection significantly counteracted the reduction in STAT3 mRNA and protein levels caused by DFOG (Fig. 6B and C).

miR-152-3p mimic suppresses the transcriptional activity of STAT3. To determine whether miR-152-3p directly targets STAT3, a luciferase reporter assay was conducted in H460-derived SFCs to identify the specific binding site of the miR-152-3p seed sequence on the 3'-UTR of STAT3 mRNA. RNAhybrid predicted binding sites for miR-152-3p and STAT3 (Fig. 7A). As shown in Fig. 7B, luciferase activity was reduced in cells co-transfected with the miR-152-3p mimic and STAT3-3'-UTR-WT, while no change in luciferase activity was observed following co-transfection with STAT3-3'-UTR-MUT. Additionally, the luciferase activity was further decreased in NSCLC cells co-transfected with miR-152-3p mimic and STAT3-3'-UTR-WT after DFOG (5 μM) treatment, compared with cells treated with miR-152-3p mimic or DFOG alone (Fig. 7C). These results demonstrated that DFOG inhibited self-renewal by upregulating miR-152-3p, which directly suppressed STAT3 expression by disrupting its transcriptional activity (Fig. 7D).

DFOG halts self-renewal in A549-derived SFCs. The inhibitory effect of DFOG on self-renewal was also assessed in A549-derived SFCs. Consistently, DFOG dose-dependently increased miR-152-3p expression, and downregulated STAT3 mRNA expression and p-STAT3 protein levels in A549 cells (Fig. 8A-C). Additionally, sphere formation (Fig. 8D) and colony formation (Fig. 8E) rates, as well as the expression of the stem cell markers CD44 and CD133 (Fig. 8F), and the pluripotent factors Oct4 and Sox2 (Fig. 8G), were all suppressed. These results indicated that DFOG-induced inhibition of self-renewal in A549-derived SFCs was mediated through the upregulation of miR-152-3p, and the suppression of STAT3 mRNA and activity.

Discussion

The present study provided evidence that DFOG inhibited self-renewal and tumor growth in NSCLC cells by upregulating miR-152-3p, thereby suppressing the expression and activity of STAT3. These findings have substantial implications for the potential use of DFOG as a therapeutic strategy for human NSCLC, particularly targeting cancer cells with self-renewal-related stemness properties.

Dysregulated miRNA expression contributes to the progression of breast cancer, liver cancer and lung cancer (31,35-37,40,41). Reduced miR-152-3p expression has been linked to multiple aspects of malignancy, including progression, proliferation, invasion and metastasis, in colon cancer, breast cancer, prostate cancer and ovarian cancer (22-25). However, further investigation is required, particularly in lung cancer. Our results demonstrated that DFOG upregulated miR-152-3p, miR-34a-5p and miR-148a-3p, with miR-152-3p exhibiting the most pronounced increase. To the best of our knowledge, the present study was the first to report that DFOG enhanced self-renewal and tumor growth traits in NSCLC cells by elevating miR-152-3p expression, thus revealing a novel mechanism through which DFOG exerts its inhibitory effects on self-renewal and tumor growth. Furthermore, the molecular mechanisms underlying DFOG-induced suppression of tumor cells involve multiple signaling pathways, including the inactivation of FoxM1 and NF-κB (17,18). One study indicated that the expression of miR-152 and STAT3 was associated with poor prognosis in epithelial ovarian cancer (31). STAT3, an oncogenic transcription factor mediating signaling from the cell surface to the nucleus, is frequently upregulated in various malignancies, including NSCLC (29,30). Notably, targeting STAT3 has been shown to reduce tumor stem cell properties (30,41,42). In the present study, a luciferase reporter assay identified STAT3 as a direct target of miR-152-3p. This finding was further corroborated by the reduced transcription of STAT3 following combined treatment with DFOG and a miR-152-3p mimic in H460-derived SFCs. The present results demonstrated that DFOG-induced upregulation of miR-152-3p inhibited self-renewal and tumor growth by downregulating STAT3 expression at the mRNA level and impairing its activity, as evidenced by decreased p-STAT3 protein levels in H460-derived SFCs. Overexpression of STAT3 reversed this effect, highlighting the interconnection among DFOG, miR-152-3p and STAT3. Collectively, these findings suggested that the inhibitory effects of DFOG on self-renewal and tumor growth were mediated through miR-152-3p upregulation and STAT3 downregulation, underscoring its potential as a preventive and therapeutic agent for NSCLC, particularly in targeting self-renewing tumor cells.

In conclusion, the present study elucidated the mechanism by which DFOG targeted STAT3 through miR-152-3p upregulation, effectively suppressing self-renewal and tumor growth in NSCLC. Therefore, DFOG may be a promising candidate for novel preventive and therapeutic interventions for NSCLC in humans.

Acknowledgements

Not applicable.

Funding

The present study was funded by the Science and Technology Innovation Leading Academics of National High-level Personnel of Special Support Program from Ministry of Science and Technology, P.R. China (grant no. GKFZ-2018-29), Department of Science and Technology of Guizhou Province [grant no. QKHJC-ZK(2022)-YB-666], and the Natural Science Foundation of Hunan Province (grant no. 2021JJ30462).

Availability of data and materials

The data generated in the present study may be requested from the corresponding author.

Authors' contributions

QY, XL and XC conducted the experiments, contributed to data collection and drafted the manuscript. JX and JZ performed the data analysis and contributed to the study design. XL, XC and JX provided resources. JZ and QY confirm the authenticity of all the raw data. All authors have read and approved the final version of the manuscript.

Ethics approval and consent to participate

All animal studies were approved (approval no. D2023045) by the Ethics Committee of Hunan Normal University (Changsha, China).

Patient consent for publication

Not applicable.

Competing interests

The authors declare that they have no competing interests.

References

1. Siegel RL, Miller KD, Fuchs HE and Jemal A: Cancer statistics, 2022. CA Cancer J Clin 72: 7-33, 2022.
2. Chansky K, Detterbeck FC, Nicholson AG, Rusch VW, Vallières E, Groome P, Kennedy C, Krasnik M, Peake M, Shemanski L, *et al*: The IASLC lung cancer staging project: External validation of the revision of the TNM stage groupings in the eighth edition of the TNM classification of lung cancer. J Thorac Oncol 12: 1109-1121, 2017.
3. Wang C, Wu Y, Shao J, Liu D and Li W: Clinicopathological variables influencing overall survival, recurrence and post-recurrence survival in resected stage I non-small-cell lung cancer. BMC Cancer 20: 150, 2020.
4. Wang X, Chen Y, Wang X, Tian H, Wang Y, Jin J, Shan Z, Liu Y, Cai Z, Tong X, *et al*: Stem cell factor SOX2 confers ferroptosis resistance in lung cancer via upregulation of SLC7A11. Cancer Res 81: 5217-5229, 2021.
5. Clara JA, Monge C, Yang Y and Takebe N: Targeting signalling pathways and the immune microenvironment of cancer stem cells-a clinical update. Nat Rev Clin Oncol 17: 204-232, 2020.
6. Schaal CM, Bora-Singhal N, Kumar DM and Chellappan SP: Regulation of Sox2 and stemness by nicotine and electronic-cigarettes in non-small cell lung cancer. Mol Cancer 17: 149, 2018.
7. Sunayama J, Matsuda K, Sato A, Tachibana K, Suzuki K, Narita Y, Shibui S, Sakurada K, Kayama T, Tomiyama A and Kitanaka C: Crosstalk between the PI3K/mTOR and MEK/ERK pathways involved in the maintenance of self-renewal and tumorigenicity of glioblastoma stem-like cells. Stem Cells 28: 1930-1939, 2010.
8. Nimmakayala RK, Leon F, Rachagani S, Rauth S, Nallasamy P, Marimuthu S, Shailendra GK, Chhonker YS, Chugh S, Chirravuri R, *et al*: Metabolic programming of distinct cancer stem cells promotes metastasis of pancreatic ductal adenocarcinoma. Oncogene 40: 215-231, 202.
9. Sharif T, Martell E, Dai C, Singh SK and Gujar S: Regulation of the proline regulatory axis and autophagy modulates stemness in TP73/p73 deficient cancer stem-like cells. Autophagy 15: 934-936, 2019.
10. Kaufhold S, Garbán H and Bonavida B: Yin Yang 1 is associated with cancer stem cell transcription factors (SOX2, OCT4, BMI1) and clinical implication. J Exp Clin Cancer Res 35: 84, 2016.
11. Walcher L, Kistenmacher AK, Suo H, Kitte R, Dluczek S, Strauß A, Blaudszun AR, Yevsa T, Fricke S and Kossatz-Boehlert U: Cancer stem cells-Origins and biomarkers: Perspectives for targeted personalized therapies. Front Immunol 11: 1280, 2020.
12. Fu Z, Cao X, Yang Y, Song Z, Zhang J and Wang Z: Upregulation of FoxM1 by MnSOD overexpression contributes to cancer Stem-like cell characteristics in the lung cancer H460 cell line. Technol Cancer Res Treat 17: 1533033818789635, 2018.
13. Liu F, Cao X, Liu Z, Guo H, Ren K, Quan M, Zhou Y, Xiang H and Cao J: Casticin suppresses self-renewal and invasion of lung cancer stem-like cells from A549 cells through down-regulation of pAkt. Acta Biochim Biophys Sin (Shanghai) 46: 15-21, 2014.
14. Wei D, Yang L, Lv B and Chen L: Genistein suppresses retinoblastoma cell viability and growth and induces apoptosis by upregulating miR-145 and inhibiting its target ABCE1. Mol Vis 23: 385-394, 2017.
15. Ma CH, Zhang YX, Tang LH, Yang XJ, Cui WM, Han CC and Ji WY: MicroRNA-1469, a p53-responsive microRNA promotes Genistein induced apoptosis by targeting Mcl1 in human laryngeal cancer cells. Biomed Pharmacother 106: 665-671, 2018.
16. Zhang L, Zhang J, Gong Y and Lv L: Systematic and experimental investigations of the anti-colorectal cancer mediated by genistein. Biofactors 46: 974-982, 2020.
17. Ning Y, Xu M, Cao X, Chen X and Luo X: Inactivation of AKT, ERK and NF-κB by genistein derivative, 7-difluoromethoxyl-5,4'-di-n-octylygenistein, reduces ovarian carcinoma oncogenicity. Oncol Rep 38: 949-958, 2017.
18. Xiang HL, Liu F, Quan MF, Cao JG and Lv Y: 7-difluoromethoxyl-5,4'-di-n-octyl genistein inhibits growth of gastric cancer cells through down-regulating forkhead box M1. World J Gastroenterol 18: 4618-4626, 2012.
19. Ren W, Hou J, Yang C, Wang H, Wu S, Wu Y, Zhao X and Lu C: Extracellular vesicles secreted by hypoxia pre-challenged mesenchymal stem cells promote non-small cell lung cancer cell growth and mobility as well as macrophage M2 polarization via miR-21-5p delivery. J Exp Clin Cancer Res 38: 62, 2019.
20. Li P, Xing W, Xu J, Yuan D, Liang G, Liu B and Ma H: microRNA-301b-3p downregulation underlies a novel inhibitory role of long non-coding RNA MBNL1-AS1 in non-small cell lung cancer. Stem Cell Res Ther 10: 144, 2019.
21. Xie C, Zhu J, Jiang Y, Chen J, Wang X, Geng S, Wu J, Zhong C, Li X and Meng Z: Sulforaphane inhibits the acquisition of tobacco Smoke-induced lung cancer stem cell-like properties via the IL-6/ΔNp63α/Notch axis. Theranostics 9: 4827-4840, 2019.
22. Lai SW, Chen MY, Bamodu OA, Hsieh MS, Huang TY, Yeh CT, Lee WH and Cherng YG: Exosomal lncRNA PVT1/VEGFA axis promotes colon cancer metastasis and stemness by down-regulation of tumor suppressor miR-152-3p. Oxid Med Cell Longev 2021: 9959807, 2021.
23. Jiang CF, Xie YX, Qian YC, Wang M, Liu LZ, Shu YQ, Bai XM and Jiang BH: TBX15/miR-152/KIF2C pathway regulates breast cancer doxorubicin resistance via promoting PKM2 ubiquitination. Cancer Cell Int 21: 542, 2021.
24. Moya L, Meijer J, Schubert S, Matin F and Batra J: Assessment of miR-98-5p, miR-152-3p, miR-326 and miR-4289 expression as biomarker for prostate cancer diagnosis. Int J Mol Sci 20: 1154, 2019.
25. Lyu M, Li X, Shen Y, Lu J, Zhang L, Zhong S and Wang J: CircATRNL1 and circZNF608 inhibit ovarian cancer by sequestering miR-152-5p and encoding protein. Front Genet 13: 784089, 2022.
26. Yuan Q, Wang R, Li X, Sun F, Lin J, Fu Z and Zhang J: DNMT1/miR-152-3p/SOS1 signaling axis promotes self-renewal and tumor growth of cancer stem-like cells derived from non-small cell lung cancer. Clin Epigenetics 16: 55, 2024.
27. Zhao L, Wu X, Zhang Z, Fang L, Yang B and Li Y: ELF1 suppresses autophagy to reduce cisplatin resistance via the miR-152-3p/NCAM1/ERK axis in lung cancer cells. Cancer Sci 114: 2650-2663, 2023.
28. Huang J, Lou J, Liu X and Xie Y: LncRNA PCGsEM1 contributes to the proliferation, migration and invasion of Non-small cell lung cancer cells via acting as a sponge for miR-152-3p. Curr Pharm Des 27: 4663-4670, 2021.
29. Huang R, Wang S, Wang N, Zheng Y, Zhou J, Yang B, Wang X, Zhang J, Guo L, Wang S, *et al*: CCL5 derived from tumor-associated macrophages promotes prostate cancer stem cells and metastasis via activating β-catenin/STAT3 signaling. Cell Death Dis 11: 234, 2020.
30. Ouyang S, Li H, Lou L, Huang Q, Zhang Z, Mo J, Li M, Lu J, Zhu K, Chu Y, *et al*: Inhibition of STAT3-ferroptosis negative regulatory axis suppresses tumor growth and alleviates chemoresistance in gastric cancer. Redox Biol 52: 102317, 2022.
31. Cao Y, Shi H, Ren F, Jia Y and Zhang R: Long non-coding RNA CCAT1 promotes metastasis and poor prognosis in epithelial ovarian cancer. Exp Cell Res 359: 185-194, 2017.
32. Al-Harbi B and Aboussekhra A: Cucurbitacin I (JSI-124)-dependent inhibition of STAT3 permanently suppresses the pro-carcinogenic effects of active breast cancer-associated fibroblasts. Mol Carcinog 60: 242-251, 2021.
33. Livak KJ and Schmittgen TD: Analysis of relative gene expression data using real-time quantitative PCR and the 2(-Delta Delta C(T)) method. Methods 25: 402-408, 2001.
34. Li X, Wang L, Cao X, Zhou L, Xu C, Cui Y, Qiu Y and Cao J: Casticin inhibits stemness of hepatocellular carcinoma cells via disrupting the reciprocal negative regulation between DNMT1 and miR-148a-3p. Toxicol Appl Pharmacol 396: 114998, 2020.
35. Chen MJ, Cheng YM, Chen CC, Chen YC and Shen CJ: MiR-148a and miR-152 reduce tamoxifen resistance in ER+ breast cancer via downregulating ALCAM. Biochem Biophys Res Commun 483: 840-846, 2017.

36. He WW, Ma HT, Guo X, Wu WM, Gao EJ and Zhao YH: lncRNA SNHG3 accelerates the proliferation and invasion of non-small cell lung cancer by downregulating miR-340-5p. J Biol Regul Homeost Agents 34: 2017-2027, 2020.
37. Chen Z, Ying J, Shang W, Ding D, Guo M and Wang H: miR-342-3p regulates the proliferation and apoptosis of NSCLC cells by targeting BCL-2. Technol Cancer Res Treat 20: 15330338211041193, 2021.
38. Li YY, Tao YW, Gao S, Li P, Zheng JM, Zhang SE, Liang J and Zhang Y: Cancer-associated fibroblasts contribute to oral cancer cells proliferation and metastasis via Exosome-mediated paracrine miR-34a-5p. EBioMedicine 36: 209-220, 2018.
39. Li LW, Xiao HQ, Ma R, Yang M, Li W and Lou G: miR-152 is involved in the proliferation and metastasis of ovarian cancer through repression of ERBB3. Int J Mol Med 41: 1529-1535, 2018.
40. Chang DL, Wei W, Yu ZP and Qin CK: miR-152-5p inhibits proliferation and induces apoptosis of liver cancer cells by up-regulating FOXO expression. Pharmazie 72: 338-343, 2017.
41. Reichenbach N, Delekate A, Plescher M, Schmitt F, Krauss S, Blank N, Halle A and Petzold GC: Inhibition of Stat3-mediated astrogliosis ameliorates pathology in an Alzheimer's disease model. EMBO Mol Med 11: e9665, 2019.
42. Liu YX, Xu BW, Niu XD, Chen YJ, Fu XQ, Wang XQ, Yin CL, Chou JY, Li JK, Wu JY, *et al*: Inhibition of Src/STAT3 signaling-mediated angiogenesis is involved in the anti-melanoma effects of dioscin. Pharmacol Res 175: 105983, 2022.